第 27 卷第 5 期
2011 年 5 月

无 机 化 学 学 报
CHINESE JOURNAL OF INORGANIC CHEMISTRY

Vol.27 No.5
951-956

具有 MIL-100 和 MIL-101 结构巨孔羧酸钪配位聚合物

李彦涛 崔科会 李 佳 朱建奇 王 新 田运齐*
(辽宁师范大学功能材料化学研究所,大连 116029)

摘要: 用溶剂热方法首次以 DMF 为溶剂合成了具有 MIL-100 和 MIL-101 结构的巨孔均苯三甲酸钪(**1**)和对苯二甲酸钪(**2**)配位聚合物,通过将钯金属纳米粒子沉积到均三苯甲酸钪(**1**)的骨架结构中的方法,获得了后功能化的载有钯纳米粒子的配位聚合物孔材料 **Pd@1**,并对以上材料进行了 X-射线粉末衍射、扫描电镜、透射电镜和氮气吸附表征。

关键词: 钪; 配位聚合物; 氮气吸附; 孔材料; 钯纳米粒子
中图分类号: O614.32+1 **文献标识码**: A **文章编号**: 1001-4861(2011)05-0951-06

The Giant Pore Metal-Organic Frameworks of Scandium Carboxylate with MIL-100 and MIL-101 Structures

LI Yan-Tao CUI Ke-Hui LI Jia ZHU Jian-Qi WANG Xin TIAN Yun-Qi*
(*Institute of Chemistry for Functionalized Materials, College of Chemistry and Chemical Engineering, Liaoning Normal University, Dalian, Liaoning* 116029, *China*)

Abstract: The giant pore metal-organic frameworks of scandium trimesate (**1**) and terephthalate (**2**) with MIL-100 and MIL-101 structures are firstly synthesized under solvothermal condition. By depositing Pd nanoparticles on the framework of **1**, the post-functionalized porous MOFs of **Pd@1** were obtained. They were all characterized by X-ray powder diffraction (XRPD), SEM, TEM, IR, TGA and nitrogen adsorption studies.

Key words: scandium(Ⅲ); metal-organic frameworks; nitrogen adsorption; palladium nanoparticles

0 Introduction

Since discovery of the giant pore metal-organic frameworks (GPMOFs) of MIL-100[1] and MIL-101[2] by Ferey and his coworkers in 2004 and 2005, a great deal of attentions has been attracted from the GPMOFs. As the pioneer of GPMOFs, MIL-100 and MIL-101 characterize with the crystalline meso-pores of very high surface area and excellent thermal stability that allow the post-functionalization[3] available and the application studies, such as, molecule storage and seperation[4], drug delivery[5] and chemical catalysis[3a,6] performable. Moreover, the GPMOFs are prepared with relatively cheap organic ligands of trimesatic acid (1,3,5-benzenetricarboxylic acid or BTC) and terephthalic acid (1,4-benzenedicarboxylate or BDC) that make the industrial production could be at a level of lower cost, when compared to the ligands for other GPMOFs[7].

MIL-100 and MIL-101 structurally adopt the zeolitic MTN topology based on the supper tetrahedral building blocks of trivalent metal trimesate and terephthalate, which contain four μ_3-oxo-centered trinuclear units (M_3O) at each tetrahedron corner. Although many trivalent metallic cations [8], such as, aluminum, scandium, vanadium, iron, chromium, indium and gallium have been found to form the trigonal trimers in MOF-

收稿日期:2010-12-29。收修改稿日期:2011-02-08。
优秀博士论文作者专项资金(No.200733)资助项目。
*通讯联系人。E-mail:yqtian@lnnu.edu.cn

type compounds, only iron and chromium can react with BTC and BDC to form the MIL-100 and MIL-101 structures[1-2], while aluminum can merely react with BTC in a very narrow pH range to form the structure of MIL-100[8]. Therefore, the synthesis of other trivalent metal trimesate and terephthalate with MIL-100 and MIL-101 structures is still challenging.

As the only rare-earth element observed in a MOF-type compound with the μ_3-oxo-centered trigonal trimers[9], scandium is more expected to form MIL-100 and MIL-101 structures that are interested for strong and effective catalysts[10]. Additionally, as the lightest rare-earth element, scandium can also be expected to form lower density MOFs that could benefit to the gas-adsorption capacity, when compared to other rare-earth metals or even to other first-transition-metals. Nevertheless, the fact is that there are very few MOFs of scandium known[9-11] that indicate a hard job has to be faced in the way for obtaining such desirable GPMOFs. However, to our surprise, both of scandium trimesate (**1**) and terephthalate (**2**) with the structures of MIL-100 and MIL-101 can be facilely prepared under solvothermal condition. By post-embedding $Pd(OAc)_2$ within the framework of **1** that was then reduced solvothermally in ethanol by benzaldehyde, the Pd-nanoparticle functionalized samples of **1** with different Pd-concentrations were also obtained.

1 Experimental

1.1 Materials and measurements

All chemicals were obtained commercially and used as received without further purification (except the solvent of DMF that was dried by zeolite-A). The IR spectra were recorded (400~4 000 cm^{-1}) on a FTIR spectrometer TENSOR 27. The X-ray powder diffraction (XRPD) analyses were carried out on a Bruker D8 Advance and the TGA was performed under air stream with a heating rate of 5 ℃·min^{-1} by using a Perkin-Elmer Diamond Thermogravimetric Analyzer. SEM images were taken by using SUPERSCAN SSX-550 for compound **1** and KYKY-1000B for compound **2** and **Pd@1** while TEM images were taken by using JEM-2100F. The sorption isotherm for N_2 was measured at 77 K by using an automatic volumetric adsorption apparatus (AUTOSORB-1MP). Before the adsorption measurement, the guest-free samples were activated in vacuum at 150 ℃ for **1** and an ambient room-temperature for **2**, respectively.

1.2 Synthesis of $\{[Sc_3O(OH)(H_2O)_2(BTC)_2]\cdot xH_2O\cdot yDMF\}_\infty$ (1)

0.204 g (0.6 mmol) of $Sc(NO_3)_3\cdot 6H_2O$ and 0.084 g (0.4 mmol) of H_3BTC were dissolved in 15 mL of DMF. The reaction mixture was stirred at room-temperature for 30 min. Then, the mixture solution was transferred into a Teflon-lined autoclave (20 mL) and heated at 150 ℃ for 36 h. After cooling to room temperature, the white powdered product of **1** was collected by filtration, washed with DMF, and dried at room temperature to give 0.15 g (yield 85%) of compound **1** ($\{[Sc_3O(OH)(H_2O)_2(BTC)_2]\cdot xH_2O\cdot yDMF\}_\infty$, x=4.5, y=2.5). Elementary chemical analysis (ECA) for $C_{25.5}H_{37.5}N_{2.5}O_{23}Sc_3$ (M_r=881.5), Calcd. (%): C, 34.7; H, 4.25; N, 3.97; found (%): C, 35.8; H, 3.60; N, 3.25. IR (cm^{-1}, KBr): 3 438(m), 1 636(s), 1 578(s), 1 455(s), 1 383(vs), 771(w), 714(m), 608(w), 778(m).

In order to get rid of the DMF resided in the pores of compound **1**, the as-synthesized sample of **1** was solvothermally treated in ethanol at 100 ℃ for 16 h and then collected by filtration, dried at room temperature.

1.3 Synthesis of $\{[Sc_3O(OH)(H_2O)_2(BDC)_3]\cdot xH_2O\cdot yDMF\cdot z[Sc(OH)(BDC)]\}_\infty$ (2)

0.084 7 g (0.25 mmol) of $Sc(NO_3)_3\cdot 6H_2O$ and 0.043 2 g (0.260 mmol) of H_2BDC were dissolved in 15 mL of DMF. The reaction mixture was stirred at room-temperature for *ca.* 30 min. and then transferred into Teflon-lined autoclave (20 mL) and heated at 90 ℃ for 24 h. After cooling to room-temperature, about 0.07 g (yield 95%) white powdered product of **2** ($\{[Sc_3O(OH)(H_2O)_2(BDC)_3]\cdot xH_2O\cdot yDMF\cdot z[Sc(OH)(BDC)]\}_\infty$, $x\approx 3$, $y\approx 1.5$, $z\approx 0.1$) was separated by filtration, washed with DMF and dried in air at room temperature. Elementary chemical analysis (ECA) for $C_{29.3}H_{34}N_{1.5}O_{21}Sc_{3.1}$ (M_r = 882.1), Calcd.(%): C, 39.86; H, 3.85; N, 2.38; found(%): C, 37.8; H, 3.70; N, 2.05. IR (cm^{-1}, KBr): 3 385(m), 1 700~1 510(vs), 1 400(vs), 1 160(w), 1 103(w), 1 019(w), 884(w), 821(w), 757(m), 700(w), 538(m).

1.4 Preparation of Pd@1

0.2 g of a freshly activated **1** was impregnated in a 20 mL tolune solution of $Pd(OAc)_2$ (containing 0.42 g $Pd(OAc)_2$ for **Pd@1** (10%) and 0.021 g $Pd(OAc)_2$ for **Pd@1** (5%)). The mixture of powder and solution was stirred for 2 h and dried under air at room-temperature. The impregnated **1** ($Pd(OAc)_2$) was vaccumed at 30 ℃ for 4 h and then reduced with benzaldehyde under solvothermal condition in ethanol at 90 ℃ for 12 h. The formed **Pd@1** samples were recovered by filtration and evacuated in vacuum for 12 h at 150 ℃.

2 Results and discussion

2.1 Synthesis

Synthesis of **1** and **2**: Both of the scandium trimesate (**1**) and the scandium terephthalate (**2**) were synthesized under solvothermal condition in DMF. However, in order to obtain a pure phase of **2**, anhydrous DMF should be employed since too much water involved in the reaction system shall lead to generating amorphous compound or isomorpheric compounds of scandium terephthalate with unknown structures.

Preparation of **Pd@1**: In consideration of compound **1** being thermally more stable than compound **2**, we attemptted also to embed Pd nanoparticles on the framework of **1** just like those of MIL-100 (Al) and MIL-101 (Cr)[12]. Unlike the method reported in literature[12], we loaded Pd nanoparticles into compound **1** by liquid reduction of $Pd(OAc)_2$ with benzaldehyde under solvothermal condition in ethanol. Two Pd@1 samples with Pd concentration of 10wt% and 5wt% were prepared, but they were finally obtained as the samples with Pd concentration of 6.6wt% and 4.5wt%, respectively (the Pd concentrations were determined by an inductively coupled plasma optical emission spectrometer (ICP-OES)).

2.2 Characterizations

Characterization of **1** and **2**: The products of **1** and **2** are characterized by SEM, XRPD, IR and nitrogen adsorption isotherms. The SEM images (Fig.1) reveal that compound **1** consists of polyhedral crystals in nano size while **2** consists of octahedral crystals in micro size. X-ray powder diffraction (XRPD) studies demonstrte that both of the compounds **1** and **2** have the desirable structures of MIL-100 and MIL-101 (Fig.2) although the diffraction peaks of each compound were observed with the small left-shift comparing to those of MIL-100 (Fe) and MIL-101 (Cr), respectively. We assign the left-shift to the unit cell swelling that arises from the M-O bond expansion between the metal ions and the carboxylic groups (normally, Sc-O bond at ~0.210 nm and Cr-O(or Fe-O) bond at ~0.200 nm). Based on the diffrac-tion data of the compound **1** and **2**,

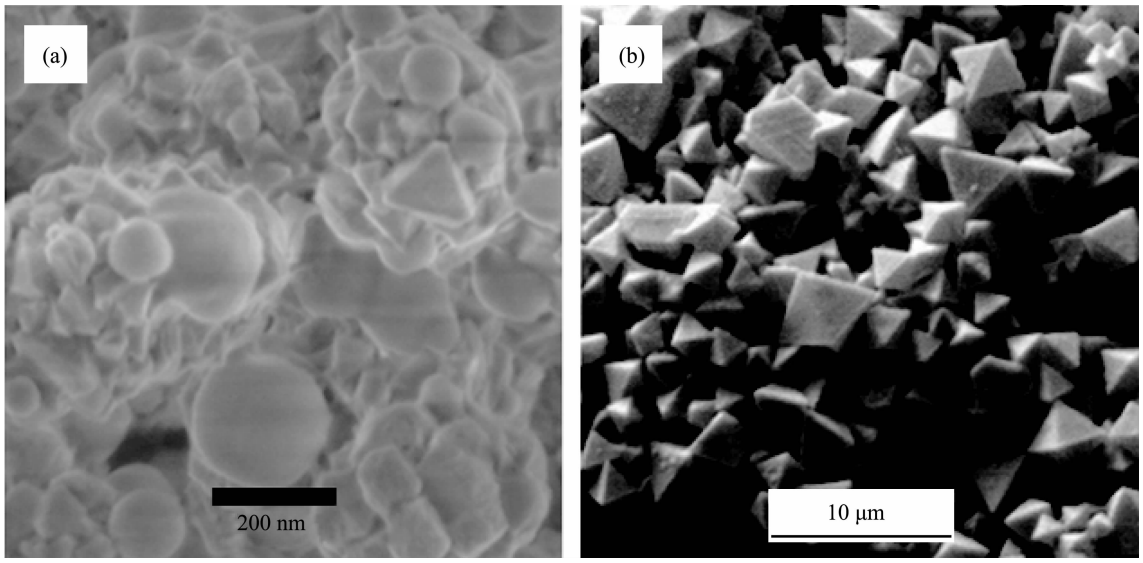

Fig.1 SEM images of compounds **1** and **2**: (a) polyhedral crystals of compound **1** with the sizes of 50~100 nm; (b) Octahedral crystals of compound **2** with the sizes of 2~5 μm

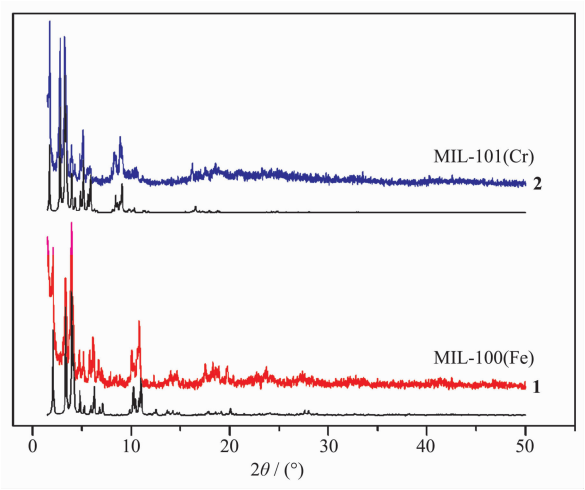

Fig.2 XRPD patterns of compound **1** compared with that of MIL-100 (Fe) (bottom) and compound **2** compared with that of MIL-101 (Cr) (top)

the cubic unit cell dimension is estimated at a=7.435 nm for **1** that is about 0.20 nm larger than the one of MIL-100 (Fe) (a=7.234 nm) and a=9.032 0 nm for **2** that is about 0.15 nm larger than that of MIL-101 (Cr) (a= 8.886 9 nm).

Accordingly, the guest-free products of **1** and **2** can be realized by solvothermal treatment of the as-synthesized samples in ethanol. Their MIL-100 and MIL-101 structures were proved being still in existence according to the XRPD patterns in agreement with those of the as-synthesized samples. It should be noticed here that the XRPD pattern of activated compound **2** shows even better resolution than the one of the as-synthesized sample due to the pores of the as-synthesized **2** are filled not only with the molecules of water and DMF, but also the unreacted therephthalic acid that can be identified from its IR spectroscopy with broad $\nu_{C=O}$ band at 1 700~1 510 cm^{-1}.

Performed on the as-synthesized samples of **1** and **2**, the thermogravimetric analyses (TGA) exhibit four and three steps of weight loss for compound **1** and **2**, respectively (see supporting Information). The weight loss below 140 ℃ assigns to the departure of free water and DMF molecules, while the weight loss between 140 and 270 ℃ is related to the removal of coordinated water molecule on the scandium. and the weight loss from 340 to 540 ℃ refers to elimination of the BTC and BDC ligands together with the collapse of the GPMOFs. Up 540 ℃, the final product of Sc_2O_3 is formed. However, for compound **1**, there is an additional weight loss between 270 and 340 ℃, corresponding to the loss of DMF molecules accommodated in the super tetrahedron of compounds **1**. Nevertheless, monitoring with the XRPD measurements, one can see that the decomposition temperature for compound **1** at 270 ℃, while for compound **2** at a temperature below 100 ℃.

Nitrogen adsorption/desorption isotherms at 77 K were measured on the guest-free samples with the activation temperature for **1** at 150 ℃ and for **2** at an ambient room-temperature (Fig.3) that show the similar curves with those of their isostructural solids of MIL-100 (Fe, Cr and Al) and MIL-101 (Cr), respectively. BET surface area (p/p_0 range 0.01~0.2, p_0 =101.325 kPa) and Langmuir surface area (p/p_0 range 0.05~0.2) of 2 400 and 3 290 $m^2 \cdot g^{-1}$ for **1** and 3 490 and 4 970 $m^2 \cdot$

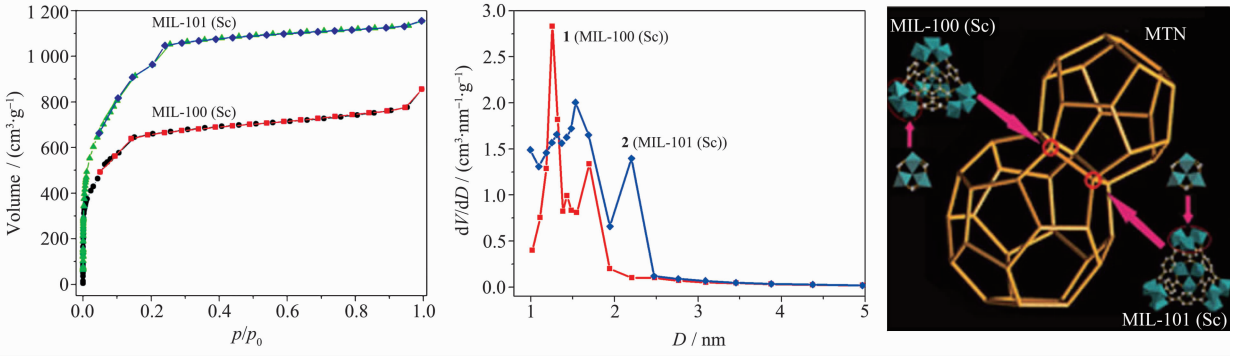

Fig.3 (a) N_2 adsorption isotherm at 77 K (p_0=101.325 kPa); (b) Pore-size distribution of **1** (MIL-100 Sc) and **2** (MIL-101 Sc); (c) Schematic view of MTN topology constructed from the super tetrahedral unit of scandium trimesate and terephthalate

g^{-1} for **2** are observed. The values for **1** are in agreement with those of the isostructural solids of MIL-100 (Cr, Fe and Al), but the values for **2** are obviously lower than those of MIL-101 (Cr) because it was measured from a sample that was insufficiently activated. The pore size distributions of **1** and **2** are measured using BJH equiliberium model that show two different pores for each compound, they are 1.26 and 1.70 nm for **1** and 1.55 and 2.21 nm for **2**, respectively. These data are almost the same as those for MIL-100(Cr) and MIL-101 (Cr) reported by Ferey et al.[22].

Characterization of **Pd@1**: the samples of **1** embeded with Pd nanoparticles were also characterized by SEM, TEM, XRPD and nitrogen gas adsorption isotherms. In view of the SEM image of the sample for **Pd@1** (4.5% Pd), one can only see the Pd nanopar-ticles in size of *ca.* 10 nm deposited on the surface of crystals of 1. But in view of the TEM image, besides the Pd nanoparticles in size of *ca.* 20 nm, one can also see the Pd nanoparticles in the size of *ca.* 2~5 nm which were deposited within the pores of compound **1** (Fig.4).

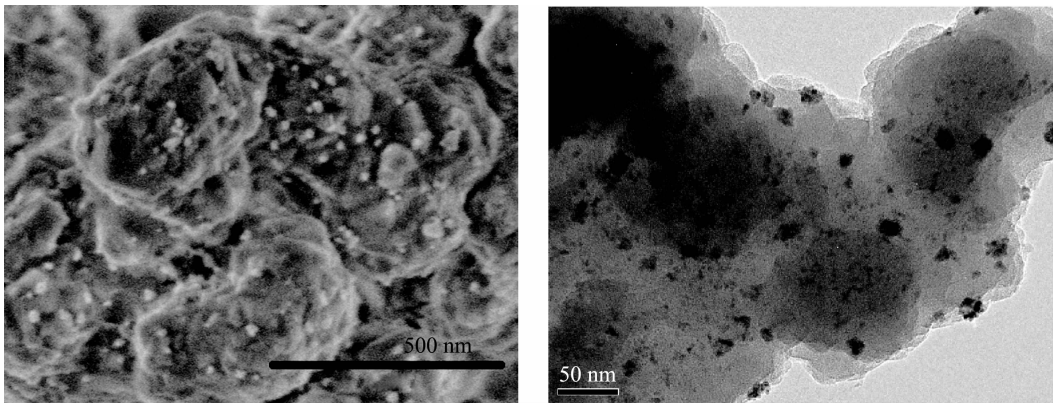

Fig.4　SEM (left) and TEM (right) images of **Pd@1** (4.5% Pd)

Compared of the XRPD patterns (Fig.5) of **Pd@1** samples with that of the as-synthesized **1**, the diffraction peaks referring to MIL-100 (Sc) structure of **1** can be observed in both of **Pd@1** (6.6% Pd) and **Pd@1** (4.5% Pd) samples that reveals the MIL-100 (Sc) structure still in existance. And in addition to those diffractions, weak broad diffractions referring to metallic Pd (fcc crystal structure) can also be observed in both of the samples that indicates the upload of Pd nanoparticles on the frameworks of **1** being achieved.

Nitrogen adsorption isotherms were also determined for the samples of **Pd@1** at 77 K that shows the surface areas and pore volumes of 1 980 $m^2 \cdot g^{-1}$ and 1.01 $cm^3 \cdot g^{-1}$ for **Pd@1** (4.5%) and 1 120 $m^2 \cdot g^{-1}$ and 0.64 $cm^3 \cdot g^{-1}$ for **Pd@1** (6.6%), respectively (Fig.6). The appreciable decrease in surface areas and pore volumes indicates that the cavities of **1** are occupied by highly dispersed Pd nanoparticles or/and blocked by the Pd

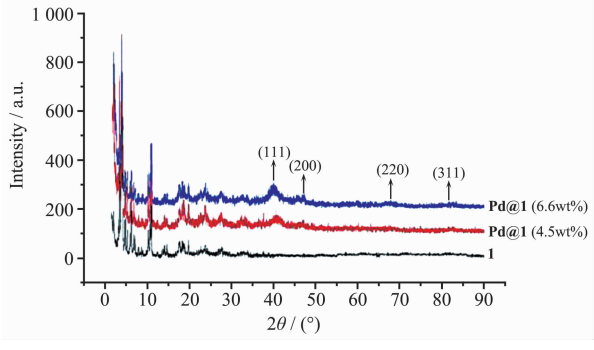

Fig.5　XRPD patterns of **Pd@1** (6.6 wt% and 4.5 wt%) and **1**

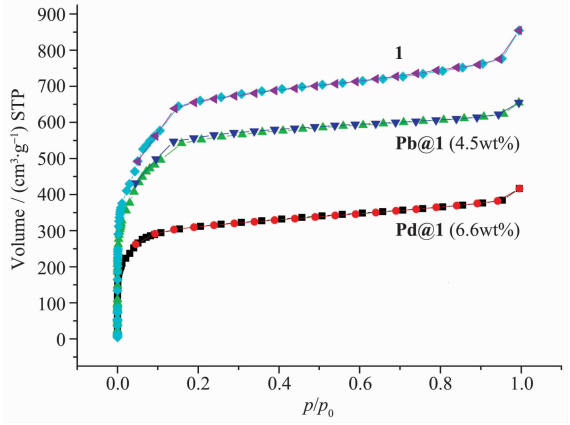

Fig.6　N_2 adsorption isotherms at 77 K (p_0=101.325 kPa) of **Pd@1** (6.6wt% and 4.5wt%) and **1**

nanoparticles that are located on the surface. Never theless, the pore size distribution curves (calculated by the BJH equation) demonstrates that the introduction of Pd nanoparticles leads to a slight reduction of the pore sizes.

In conclusion, scandium trimesate (**1**) and terephthalate (**2**) with MIL-100 and MIL-101 structures have been successfully synthesized under solvothermal condition in DMF. The scandium trimesate (**1**) (MIL-100 (Sc)) exhibits the porosity of BET surface area of 2 400 $m^2 \cdot g^{-1}$ and the thermal stability of 270 ℃ that is post-functionalizationally superior to the scandium terephthalate (**2**) (MIL-101 (Sc) with the BET surface area of 3 490 $m^2 \cdot g^{-1}$ and thermal stability below 100 ℃. By uploadding Pd nanoparticles on the framework of MIL-100 (Sc), **Pd@1** samples with Pd concentration of 6.6wt% and 4.5wt% were obtained. Characterized with the effective porosity and the almost unchanged pore sizes, the **Pd@1** is applicable for the Pd nanoparticle-catalyzed reactions, on which a corresponding study is in process.

References:

[1] Ferey G, Serre C, Mellot-Draznieks C, et al. *Angew. Chem. Int. Ed.*, **2004**,**43**:6296-6301

[2] Férey G, Mellot-Draznieks C, Serre C, et al. *Science*, **2005**, **309**:2040-2042

[3] (a)Banerjee M, Das S, Yoon M, et al. *J. Am. Chem. Soc.*, **2009**, **131**:7524-7525

(b)Pan Y, Yuan B, Li Y, et al. *Chem. Commun.*, **2010**,**46**:2280-2282

(c)Hong D Y, Hwang Y K, Serre C, et al. *Adv. Funct. Mater.*, **2009**,**19**:1537-1552

(d)Zlotea C, Campesi R, Cuevas F, et al. *J. Am. Chem. Soc.*, **2010**,**132**:2991-2997

[4] (a)Latroche M, Surbl S, Serre C, et al. *Angew. Chem. Int. Ed.*, **2006**,**45**:8227-8231

(b)Liu Y Y, Zeng J L, Zhang J, et al. *Intern. J. Hydro. Ener.*, **2007**,**32**:4005-4010

(c)Gu Z Y, Yan X P. *Angew. Chem. Int. Ed.*, **2010**,**49**:1477-1480

[5] (a)Taylor-Pashow K M L, Rocca J D, Xie Z, et al. *J. Am. Chem. Soc.*, **2009**,**131**:14261-14263

(b)Horcajada P, Chalati T, Serre C, et al. *Nat. Mater.*, **2010**,**9**:172-178

[6] (a)Horcajada P, Surblé S, Serre C, et al. *Chem. Commun.*, **2007**:2820-2822

(b)Juan-Alcaniz J, Ramos-Fernandez E V, Lafont U, et al. *J. Cat.*, **2010**,**269**:229-241

(c)Henschel A, Gedrich K, Kraehnert R, et al. *Chem. Commun.*, **2008**:4192-4194

(d)Kim J, Bhattacharjee S, Jeong K E, et al. *Chem. Commun.*, **2009**:3904-3906

[7] (a)Sonnauer A, Hoffmann F, Frba M, et al. *Angew. Chem. Int. Ed.*, **2009**,**48**:3791-3794

(b)Koh K, Wong-Foy A G, Matzger A J. *J. Am. Chem. Soc.*, **2009**,**131**:4184-4185

(c)Park Y K, Choi S B, Kim H, et al. *Angew. Chem. Int. Ed.*, **2007**,**46**:8230-8233

(d)Wang X S, Ma S, Sun D, et al. *J. Am. Chem. Soc.*, **2006**, **128**:16474-16475

(e)Ma S, Sun D, Ambrogio M, et al. *J. Am. Chem. Soc.*, **2007**, **129**:1858-1859

[8] Volkringer C, Popov D, Loiseau T, et al. *Chem. Mater.*, **2009**, **21**:5695-5697 and references therein

[9] Dietzel P D C, Blom R, Fjellvag H. *Dalton Trans.*, **2006**:2055-2057

[10](a)Perles J, Iglesias M, Ruiz-Valero C, et al. *J. Mater. Chem.*, **2004**,**14**:2683-2689

(b)Perles J, Iglesias M, Ruiz-Valero C, et al. *Chem. Commun.*, **2003**:346-347 and references therein

[11]Perles J, Iglesias M, Martín-Luengo M, et al. *Chem. Mater.*, **2005**,**17**:5837-5842

[12](a)Zlotea M, Campesi R, Cuevas F, et al. *J. Am. Chem. Soc.*, **2010**,**132**:2991-2997

(b)Pan Y, Yuan B, Li Y, et al. *Chem. Commun.*, **2010**,**46**:2280-2282